

Power-level regulation and simulation of nonlinear pressurized water reactor core with xenon oscillation using H-infinity loop shaping control

Gang Li^{1,2}, Bin Liang^{1,2,a}, Xueqian Wang^{1,2}, Xiu Li^{1,2} and Kang Wang^{1,2}

¹Tsinghua University, National Laboratory for Information Science and Technology, 100084 Beijing, China

²Shenzhen Key Lab of Space Robotic Technology and Telescience, 518055 Shenzhen, China

Abstract. This investigation is to solve the power-level control issue of a nonlinear pressurized water reactor core with xenon oscillations. A nonlinear pressurized water reactor core is modeled using the lumped parameter method, and a linear model of the core is then obtained through the small perturbation linearization way. The H ∞ loop shaping control is utilized to design a robust controller of the linearized core model. The calculated H ∞ loop shaping controller is applied to the nonlinear core model. The nonlinear core model and the H ∞ loop shaping controller build the nonlinear core power-level H ∞ loop shaping control system. Finally, the nonlinear core power-level H ∞ loop shaping control system is simulated considering two typical load processes that are a step load maneuver and a ramp load maneuver, and simulation results show that the nonlinear control system is effective.

1 Introduction

Nuclear energy as a clean energy can be sustainable and renewable. Hence, developing technologies of nuclear power plants (NPPs) for electricity generation is inevitable. Of these technologies, it is necessary to investigate the power control technology of nonlinear nuclear reactor cores with xenon oscillations.

Several researchers have made great efforts for the improvement of reactor core power control systems. The state-feedback based control with classical control part was proposed by Edwards et al. [1-2] to devise power control systems of pressurized water reactor (PWR) cores. The linear quadratic Gaussian with loop transfer recovery (LQG/LTR) control was adopted to contrive PWR core controllers for power regulations [3-4]. However, the controllers in references [1-4] are designed based on a linear core model without xenon oscillations, and not always optimal or even ineffective for nonlinear cores.

Based on this consideration, the H ∞ loop shaping control [5] with stronger robustness than that of the state-feedback or LQG/LTR control is adopted to design a nonlinear power control system of a PWR core with xenon oscillations. Finally, the nonlinear PWR core power H ∞ loop shaping control system is simulated and conclusions are drawn.

2 Modeling for PWR core

According to the point reactor core modeling [6-8], the nonlinear PWR core is modeled adopting the point kinetics equations with six groups of delayed neutrons and reactivity feedbacks due to control rod movement

and variations in fuel temperature, coolant temperature and xenon concentration. Main model parameters are given in Table 1. The nonlinear core model is showed as Eq.(1).

$$\left\{ \begin{aligned} \frac{dP_r}{dt} &= \frac{\rho - \beta}{\Lambda} P_r + \sum_{i=1}^g \frac{\beta_i c_{ri}}{\Lambda} \\ \frac{dc_{ri}}{dt} &= \lambda_i P_r - \lambda_i c_{ri}, i = 1, 2, \dots, g \\ \frac{dI_r}{dt} &= \frac{\gamma_I P_{f0}}{E_{eff} V I_{f0}} P_r - \lambda_I I_r \\ \frac{dX_r}{dt} &= \frac{\gamma_X P_{f0}}{E_{eff} V X_{f0}} P_r + \frac{\lambda_I I_{f0}}{X_{f0}} I_r - (\lambda_X + \frac{\sigma_X P_{f0}}{E_{eff} \Sigma_f V} P_r) X_r \\ \frac{dT_f}{dt} &= \frac{f_f P_0}{\mu_f} P_r - \frac{\Omega}{\mu_f} T_f + \frac{\Omega}{2\mu_f} T_i + \frac{\Omega}{2\mu_f} T_e \\ \frac{dT_e}{dt} &= \frac{(1-f_f)P_0}{\mu_c} P_r + \frac{\Omega}{\mu_c} T_f + \frac{2M - \Omega}{2\mu_c} T_i - \frac{2M + \Omega}{2\mu_c} T_e \\ \rho &= \rho_{rod} + \alpha_f (T_f - T_{f0}) + \frac{\alpha_c}{2} (T_i - T_{i0}) + \frac{\alpha_c}{2} (T_e - T_{e0}) \\ &\quad + \alpha_x X_{f0} (X_r - X_{r0}) \\ \delta \rho_{rod} &= \alpha_{rod} \delta rod \end{aligned} \right. \quad (1)$$

^a Corresponding author: wychug@163.com

Table 1. Main model parameters.

Parameter	Name
P_r	core power level
c_{ri}	i th group normalized precursor concentration
c_r	normalized precursor concentration
I_r	normalized iodine concentration
X_r	normalized xenon concentration
T_f	fuel average temperature
T_i	coolant inlet temperature
T_e	coolant outlet temperature
δrod	position variation of the control rod (fraction of core length)
δ	deviation of a parameter from initial steady-state value

One group delayed neutron model is utilized and the coolant inlet temperature is treated as a constant [2-4]. The small perturbation linearization methodology is utilized to linearize the nonlinear core model (1). The transfer function and the state equation of the core are separately calculated and expressed by

$$G = \frac{\delta P_r}{\delta rod} = \frac{\sum_{i=0}^5 a_i s^i}{\sum_{i=0}^6 b_i s^i} \quad (2)$$

$$\begin{cases} \dot{\mathbf{x}} = \mathbf{A}\mathbf{x} + \mathbf{B}u \\ y = \mathbf{C}\mathbf{x} + \mathbf{D}u \end{cases} \quad (3)$$

where $u = \delta rod$ -the input; $y = \delta P_r$ -the output; a_i ($i=0,1,2,5$)-numerator coefficients; b_i ($i=0,1,2,3,6$)-denominator coefficients; s -laplace operator; $\mathbf{x} = [x_1, x_2, x_3, x_4, x_5, x_6]^T = [\delta P_r, \delta c_r, \delta I_r, \delta X_r, \delta T_f, \delta T_e]^T$ -the state matrix; \mathbf{A} -the $\mathbb{R}^{6 \times 6}$ system matrix; \mathbf{B} -the $\mathbb{R}^{6 \times 1}$ input matrix; \mathbf{C} -the $\mathbb{R}^{1 \times 6}$ output matrix; \mathbf{D} -the zero matrix.

The transfer function G is calculated by using parameters from Ref. [9], in which the total primary heat output is 2200 MW, the primary coolant inlet temperature is 285°C, the primary coolant outlet temperature is 317°C, the primary coolant average pressure is 15.5 MPa, and the primary coolant mass flow is 12861.1 kg/s.

3 H_∞ loop shaping control

The H_∞ loop shaping design approach was proposed by McFarlane et al. [5] to implement tradeoffs between performance and robust stability of a stable H_∞ loop shaping control system for a plant, where a normalized coprime factor H_∞ robust stabilization issue needs to be

solved to guarantee closed-loop stability and a certain level of robust stability of the system at all frequencies.

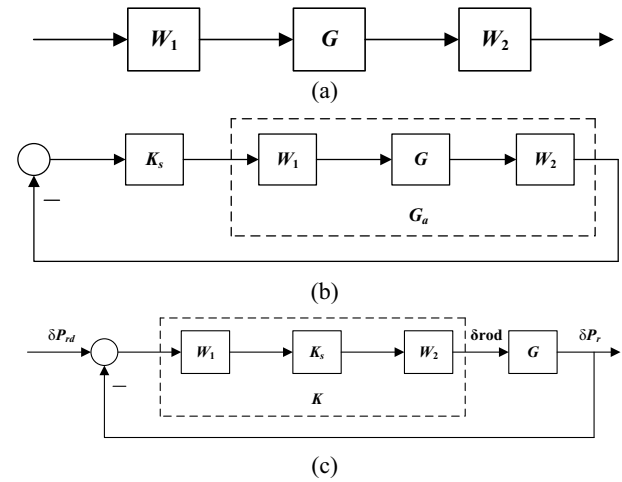


Figure 1. The loop shaping design procedure for the core.

This H_∞ loop shaping design approach consists of two key techniques, namely loop shape and robust stabilization. The loop shaping design procedure is shown in Fig.1, where W_1 and W_2 are weight matrices or compensators; G_a is a shaped plant based on G ; K_s is the H_∞ controller of G_a ; K is the controller to be devised; $\delta P_{r,d}$ denotes the reference input, namely the desired change of power level.

(1) Loop shaping

Singular values of a controlled plant G are regulated to obtain a desired open loop shape adopting an additional pre-compensator W_1 and/or an additional post-compensator W_2 . The plant G is shaped to be G_a introducing W_1 and/or W_2 , $G_a = W_2 G W_1$. Suppose W_1 and W_2 are such that G_a contains no hidden modes with instability.

(2) Robust stabilization

Step one: Calculation of \mathcal{E}_{\max}

$$\mathcal{E}_{\max} = \left[\inf_{K \text{ stabilizing}} \left\| \begin{bmatrix} I \\ K \end{bmatrix} (I - G_a K)^{-1} M_s^{-1} \right\|_{\infty} \right]^{-1} \quad (4)$$

where M_s is a normalized coprime factor of G_a subjecting to $G_a = M_s^{-1} N_s$.

Step two: Select $\mathcal{E} \leq \mathcal{E}_{\max}$, design a stabilizing controller K_s satisfying

$$\left\| \begin{bmatrix} I \\ K_s \end{bmatrix} (I - G_a K_s)^{-1} M_s^{-1} \right\|_{\infty} \leq \mathcal{E}^{-1} \quad (5)$$

(3) The eventual feedback controller: $K = W_1 K_s W_2$.

The stability margin \mathcal{E} is both a measurement for robustness of a loop shape control system and the indicator of the success of the loop shaping. Generally speaking, K_s is solved so that $\mathcal{E} \leq \mathcal{E}_{\max}$ and the controller

can guarantee that the control system possess satisfied robustness. A small value of \mathcal{E}_{\max} indicates incompatibility among a desired loop shape, a controlled plant and closed-loop robust stability. In the presence of this case, W_1 and W_2 need to be regulated again to obtain a decent loop shape.

4 Design of nonlinear PWR core power control system

According to Section 3, solving K is the following.

(1) Loop shaping

G_a is exploited and defined as a shaped plant of G . Of selected weight matrices for G , W_1 is $I_{1 \times 1}$; W_2 is expressed by Eq.(6), and parameters of W_2 are shown in Table 2, where $e^i=10^i$.

$$W_2 = \frac{\sum_{i=0}^6 c_i s^i}{\sum_{i=0}^6 d_i s^i} \quad (6)$$

Table 2. Parameters of W_2 .

Weight matrix	$[c_6 \ c_5 \ c_4 \ c_3 \ c_2 \ c_1 \ c_0]$ $[d_6 \ d_5 \ d_4 \ d_3 \ d_2 \ d_1 \ d_0]$
W_2	$[10 \ 4014 \ 6921 \ 3898 \ 432.1 \ 0.03186 \ 1.42e-6]$ $[5088 \ 7032 \ 1868 \ 141.2 \ 0.2974 \ 4.531e-5 \ 8.151e-10]$

(2) Solve controllers

The controller K_s is solved, and then the final controller K of G is calculated by $K=W_1K_sW_2$. K is expressed by Eq.(7), and parameters of K of G are shown in Table 3. The solved stability margin \mathcal{E} of K is shown in Table 3.

$$K = \frac{\sum_{j=0}^{11} e_j s^j}{\sum_{j=0}^{12} f_j s^j} \quad (7)$$

Table 3. Parameters of K .

Controller	$[e_{11} \ e_{10} \ e_9 \ e_8 \ e_7 \ e_6 \ e_5 \ e_4 \ e_3 \ e_2 \ e_1 \ e_0]$ $[f_{12} \ f_{11} \ f_{10} \ f_9 \ f_8 \ f_7 \ f_6 \ f_5 \ f_4 \ f_3 \ f_2 \ f_1 \ f_0]$
K	$[8.06 \ 3.625e4 \ 1.326e7 \ 2.288e7 \ 1.291e7 \ 1.452e6 \ 2960 \ 2.525 \ 0.001146 \ 2.914e-7 \ 3.925e-112.184e-15]$ $[1 \ 8213 \ 1.687e7 \ 2.334e7 \ 6.233e6 \ 4.79e5 \ 1839 \ 2.546 \ 0.001786 \ 7.093e-7 \ 1.62e-10 \ 1.987e-14 \ 1.015e-18]$

(3) Effect of local controllers

When the reference input δP_{rd} is taken as a 0.1 step, responses of the output δP_r in G with K are shown in Fig.2, where the curve is step response of δP_r in G with K . According to the curve, the output δP_r in G with K in response to a step possesses good performance, such as

the zero overshoot, the short adjustment time and the zero static error. Hence, the controller K is desirable.

The solved controller K is applied to the nonlinear core model. The combination of the nonlinear core model and K is the nonlinear core power H_∞ loop shaping control system. The schematic of the nonlinear core power H_∞ loop shaping control system is shown in Fig.3.

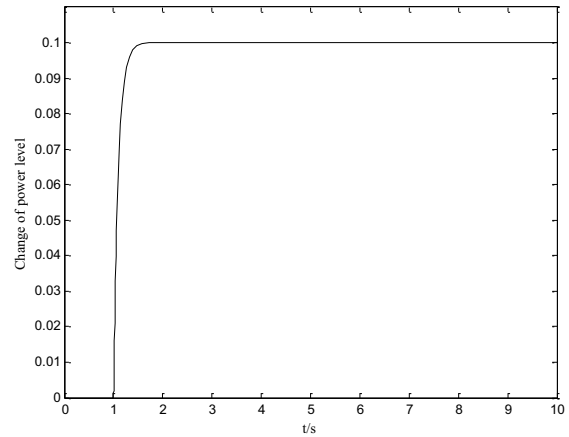


Figure 2. Step response of the output δP_r from G_i with K_i ($i=1, \dots, 7$).

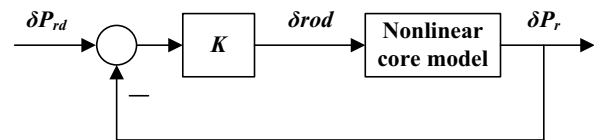


Figure 3. Schematic of the nonlinear core power H_∞ control system.

5 Simulations

The nonlinear core power H_∞ loop shaping control system is simulated considering two typical load variations that are the -10% step process and the ramp process with $\pm 0.0556\% \cdot \text{min}^{-1}$ variations. The direction from the bottom to the top of core is treated as the positive direction of y-axis for simulation work, the core bottom is the zero point of y-axis and the height of core is 366cm. When the core power level is at 100%, the initial rod position is at the top of the core, namely at 366cm.

When the reference input δP_{rd} is taken as a -10% step load in 24 hours, change trajectories of core parameters during the core following the step load (100%→90%) are shown in Fig.4, where S1 is the desired load change trajectory for the start of reactor full power level operation, the middle of reactor shut-down operation with a -10% step variation, and the end of 90% power level operation; S2 is a change trajectory of the core power level; S3 is a change trajectory of the control rod position in the core.

When the reference input δP_{rd} is taken as a ramp load with $\pm 0.0556\% \cdot \text{min}^{-1}$ variations, change trajectories of core parameters during the core following the ramp load (100%→90%→100%) are shown in Fig.5, where R1 is the desired load change trajectory for the start of reactor full power level operation, the middle of reactor shut-down operation with a $-6\% \cdot \text{min}^{-1}$ ramp variation and 90% power level operation, and the end of reactor start-up operation with a $6\% \cdot \text{min}^{-1}$ ramp variation; R2 is a change

trajectory of the core power level; R3 is a change trajectory of the control rod position in the core.

Consequently, SL2 (RL2) can follow SL1 (RL1) in real time; meanwhile, the processes of SL3 and RL3 are suitable and acceptable.

Hence, S2 can follow S1, and R2 can follow R1 in real time. Besides, the dynamic processes of S3 and R3 are acceptable.

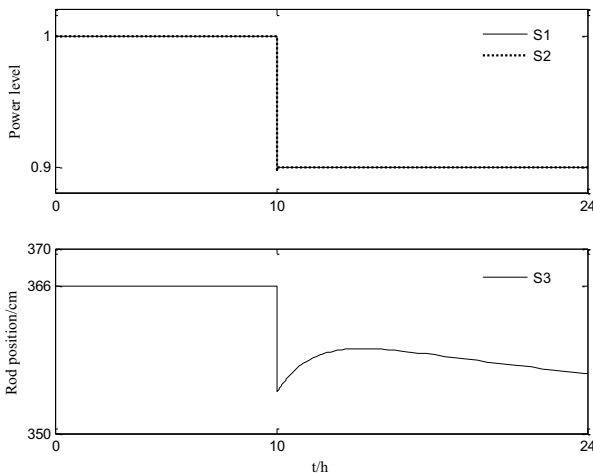


Figure 4. Change trajectories of core parameters during the core following a step load (100%→90%).

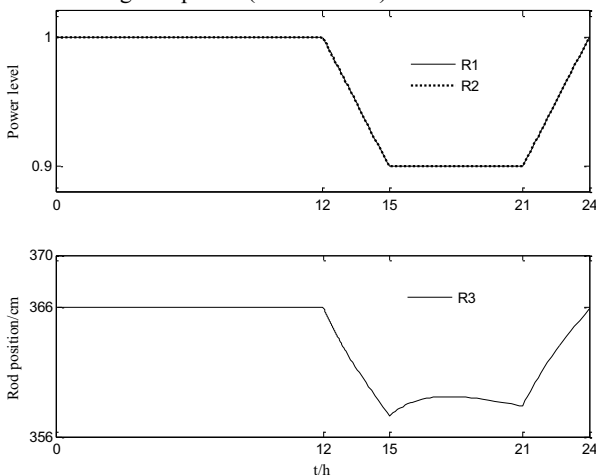


Figure 5. Change trajectories of core parameters during the core following a ramp load (100%→90%→100%).

6 Conclusions

The power-level control for PWR cores with xenon oscillations is difficult to be implemented, which is also a challenge research direction. In this paper, the power-

level control problem for a PWR core is handled applying the H_∞ loop shaping control strategy to this nonlinear core.

The nonlinear PWR core and its linearized model are separately modeled using the lumped parameter method and the small perturbation linearization method that are capable of being reference modeling approaches to study other nonlinear plants.

In order to implement applications of the controller designed on a linearized core model to a nonlinear core model, the solved H_∞ loop shaping controller has strong robustness of accommodating model errors between the nonlinear model and the linear model.

The devised nonlinear PWR core power H_∞ loop shaping control system can control the core power level satisfactorily in response to different load changes such as a step or ramp. Hence, the nonlinear PWR core power H_∞ loop shaping control system is effective.

Acknowledgement

The authors would like to thank anonymous reviewers for their valuable comments. The work is funded by National High Technology Research and Development Program of China (863 Program) (No.2015AAXX46611) and China Postdoctoral Science Foundation (No.20159200078).

References

1. R. M. Edwards, *Robust optimal control of nuclear reactors* (Pennsylvania State University, 1991)
2. R. M. Edwards, K. Y. Lee, M. A. Schultz, *Nuclear Technology*, **92**, 167-185 (1990).
3. A. Ben-Abdennour, R. M. Edwards, K. Y. Lee, *IEEE Trans. on Nuclear Science*, **39**, 2286-2294 (1992).
4. H. Arab-Alibeik, S. Setayeshi, *IEEE Trans. on Nuclear Science*, **50**, 211-218 (2003).
5. D. McFarlane, K. Glover, *IEEE Trans. on Autom. Control*, **37**, 759-769 (1992).
6. M. A. Schultz, *Control of nuclear reactors and power plants* (McGraw-Hill, 1961).
7. T. W. Kerlin, E. M. Katz, J. G. Thakkar, J.E. Strange, *Nuclear Technology*, **30**, 299-316 (1976).
8. M. N. Khajavi, M. B. Menhaj, A. A. Suratgar, *Annals of Nuclear Energy*, **29**, 751-760 (2002).
9. IAEA, *Directory of Nuclear Reactors Vol.IX*, (International Atomic Energy Agency, 1971).